ARTICLE

Predictions of Systemic, Intracellular, and Lung Concentrations of Azithromycin With Different Dosing Regimens Used in COVID-19 Clinical Trials

Jim H. Hughes[1], Kevin Sweeney[1], Sima Ahadieh[1] and Daniele Ouellet[1,2,*]

Azithromycin (AZ), a broad-spectrum macrolide antibiotic, is being investigated in patients with coronavirus disease 2019 (COVID-19). A population pharmacokinetic model was implemented to predict lung, intracellular poly/mononuclear cell (peripheral blood monocyte (PBM)/polymorphonuclear leukocyte (PML)), and alveolar macrophage (AM) concentrations using published data and compared against preclinical effective concentration 90% (EC_{90}) for severe acute respiratory syndrome-coronavirus 2 (SARS-CoV-2). The final model described the data reported in eight publications adequately. Consistent with its known properties, concentrations were higher in AM and PBM/PML, followed by lung tissue, and lowest systemically. Simulated PBM/PML concentrations exceeded EC_{90} following the first dose and for ~ 14 days following 500 mg q.d. for 3 days or 500 mg q.d. for 1 day/250 mg q.d. on days 2–5, 10 days following a single 1,000 mg dose, and for > 20 days with 500 mg q.d. for 10 days. AM concentrations exceeded the 90% inhibitory concentration for > 20 days for all regimens. These data will better inform optimization of dosing regimens for AZ clinical trials.

Study Highlights

WHAT IS THE CURRENT KNOWLEDGE ON THE TOPIC?
☑ Azithromycin (AZ) is currently being used in clinical trials of patients with coronavirus disease 2019 (COVID-19), although its optimal dose is unknown.

WHAT QUESTION DID THIS STUDY ADDRESS?
☑ The study was able to predict AZ concentrations in relevant tissues for antiviral activity including lung, polymorphonuclear and mononuclear cells, and alveolar macrophages using different dosing regimens and compare against *in vitro* effective concentration 90% (EC_{90})

for severe acute respiratory syndrome-coronavirus 2 (SARS-CoV-2).

WHAT DOES THIS STUDY ADD TO OUR KNOWLEDGE?
☑ Azithromycin predicted exposure exceeded target EC_{90} in relevant tissues. The analysis provides a rationale to support dosing of AZ in clinical trials using az alone or in combination with other agents.

HOW MIGHT THIS CHANGE DRUG DISCOVERY, DEVELOPMENT, AND/OR THERAPEUTICS?
☑ Results will better inform optimization of dosing regimens for clinical trials of AZ.

Azithromycin (AZ), a broad-spectrum macrolide antibiotic with a long half-life and extensive tissue distribution, is being investigated in multiple clinical trials in patients with coronavirus disease 2019 (COVID-19; clinicaltrials.gov). An early uncontrolled clinical study in a small number of patients showed that AZ combined with hydroxychloroquine contributed to the reduction in viral load in patients with COVID-19.[1] The study was expanded to a pilot study in a total of 80 mildly infected subjects who showed clinical improvement with administration of the combined medications.[2] Controlled clinical studies in a larger number of patients are required to understand the clinical effect of AZ in this patient population. To support the planning and safe administration of AZ alone and in combination with other agents, the clinical pharmacology, activity against different

viral agents, and safety of AZ were recently reviewed by Damle *et al.*[3]

AZ is not approved for antiviral therapy, including infections with severe acute respiratory syndrome-coronavirus 2 (SARS-CoV-2), the virus causing COVID-19. However, several mechanisms have been postulated to support its activity against viral pathogens.[3] AZ is a weak base ionized at cellular pH and, thus, accumulates in intracellular compartments, more specifically in lysosomes, and remains in these cells for an extended period of time. The accumulation of ionized AZ in these cells would increase pH, altering the acidic environment required for uncoating of enveloped viruses, and potentially impairing viral replication. In a recent preclinical study, the *in vitro* 50% effective concentration and 90% effective concentration (EC_{90}) of AZ against SARS-CoV-2 was 2.12 μM

(~ 1,600 ng/mL) and 8.65 μM (~ 6,500 ng/mL), respectively, as determined in a viral assay model using VeroE6 cells.[4]

To better understand its efficacy against bacterial infections in the lungs, investigators have measured AZ in different tissues, including epithelial lining fluid, lung tissue homogenate, lung alveolar macrophages (AMs), and intracellularly in peripheral blood mononuclear cells (monocyte or lymphocyte (PBM)) or polymorphonuclear leukocyte (PML; **Table 1**).[5–13] A population pharmacokinetic (PopPK) model describing tissue distribution of unbound drug in muscle and subcutis and in PML separately for AZ un-ionized in cytosol and ionized in lysosome compartments has been developed by Zheng *et al*.,[5] based on data originally published in Matzneller *et al*.[6] This paper summarizes the extension of the PopPK model to predict tissue distribution in the lungs and AMs, as intracellular concentrations are most relevant to antiviral activity. The model can be utilized to assess the effectiveness of different dosing regimens based on comparison of the predictions in tissues to the *in vitro* antiviral EC_{90} value. Assessed regimens included those approved by the US Food and Drug Administration (FDA) for different mild to moderate bacterial infections, including 500 mg as a single dose on day 1 followed by 250 mg q.d. on days 2 through 5; 500 mg once daily for 3 days; and 1,000 or 2,000 mg as a single dose in adults.

METHODS
Model development
For the current analysis, model development and simulations were undertaken using the following steps, which are further described below.

1. Internalize model developed by Zheng *et al*., to simulate concentrations in plasma, muscle/subcutis, and PML;
2. Perform external visual predictive checks (VPCs) for plasma/serum and white blood cell (WBC) concentration-time profiles against mean/median and

available individual data and adjust parameters, as required;
3. Using the same model structure as Zheng *et al*. for tissue and intracellular concentrations, add parameters to describe published lung and AM concentration-time data;
4. Conduct sensitivity analysis to verify assumptions around final parameter values;
5. Use the model to simulate relevant dosing regimens of AZ.

First, the AZ specific PopPK model developed by Zheng *et al*.[5] was utilized as the initial base model. This model consisted of a three-compartment model with first order absorption and elimination, with an absorption lag describing the disposition of unbound AZ in plasma, and both fast and slow equilibrating tissues (**Figure 1**). The model also included two tissue compartments one each for muscle and subcutis, and another compartment for PMLs, each with an associated deep-tissue compartment. Distribution to tissue compartments was driven by unbound drug from plasma, whereas distribution to PML cytosol was driven by unbound un-ionized drug from plasma. Tissue and cell concentrations were scaled according to estimated distribution factors representing the ratio between tissue/cell concentrations and plasma concentrations.

As reported by Zheng *et al*.,[5] the base model was fitted to free plasma concentrations, with the model data derived from total plasma concentrations (C_p) using a concentration-dependent fraction unbound (f_u) (Eq. 1):

$$f_u = 0.4984 + \frac{0.5339 \cdot C_p}{230.9 + C_p} \tag{1}$$

with f_u equal to 0.4984 at very low AZ concentration and up to 0.8 at a concentration of 300 ng/mL. A full description of the model can be found in the original publication.[5]

Second, an evaluation of the typical plasma predictions and parameter estimates of the initial base model was

Table 1 Summary of published systemic and tissue pharmacokinetics of azithromycin

	Zheng *et al.*, 2014[5] Matzneller *et al.*, 2013[6]	Sampson *et al.*, 2014[7]	Lucchi *et al.*, 2008[8]	Liu *et al.*, 2007[9]	Danesi *et al.*, 2003[10]	DiPaolo *et al.*, 2002[11]	Ballow *et al.*, 1998[12]	Olsen *et al.*, 1996[13]
Dose	500 mg D1–D3	250 and 1,000 mg SD	500 mg SD	500 mg D1–D3[c]	500 and 1,000 mg D1–D3	500 and 1,000 mg D1–D3	500 mg D1, 250 mg D2–D5	500 mg D1, 250 mg D2–D5
No. enrolled	6	10/dose	32[a]	12	24/dose[a]	28/dose[a]	14	25[a]
Plasma/serum	Plasma		Serum	Serum	Plasma	Plasma	Serum	Serum
Sampling[b]	0–7 days		0–72 hours	0–5 days	0–204 hrs	0–204 hours	0–264 hours	0–508hours
PML (poly)	X	X (PMN)		X (PMNL)			X	
PBM (mono)		X (PBMC)		X (MNL)				X
Lung			X		X	X		
AM			X					X
Other	ISF in muscle and subcutis	Blood	ELF		Bronchial washing	Bronchial washing	Urine, RBC, blister fluid	ELF

AM, alveolar macrophage; D, days; ELF, epithelial lining fluid; ISF, interstitial fluid; MNL, mononuclear leukocytes; PBM, peripheral blood monocyte; PBMC, peripheral blood mononuclear cells; PML, polymorphonuclear leukocytes; PMN, polymorphonuclear cells; PMNL, polymorphonuclear leukocytes; RBC, red blood cell.
[a]Number represents total number of subjects; N for tissue samples ranged from 3 to 6 per timepoint.
[b]Sampling time is reported relative to first dose.
[c]Another cohort of subjects received an extended release formulation.
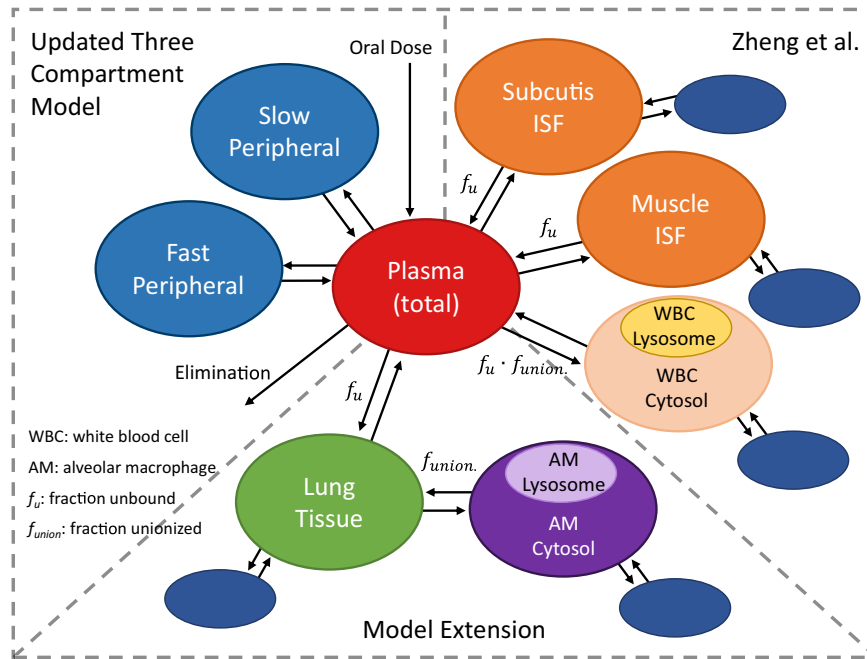
Figure 1 Structural model of azithromycin pharmacokinetics derived from Zheng *et al.*[5] and Zhao *et al.*[14]. AM, alveolar macrophage; f_u, fraction unbound; f_{union}, fraction un-ionized; ISF, interstitial fluid; WBC, white blood cell.

conducted against other AZ PopPK models in the literature (**Supplementary Table S1**)[9,12,14–17] and published summary PBM and PML data,[6,7,9,13] as defined in the section below (Data for External Validation). Changes to the initial three-compartment structure (systemic disposition) parameters were made based on comparison to other published AZ PopPK models, after adjusting for the difference in free and total concentrations. AZ PopPK models fitted to total plasma concentrations required the f_u to be incorporated when drug was distributed to the muscle, subcutis, and PML compartments of the base model (Eq. 2):

$$\frac{dA_{tis}}{dt} = k_{in} \cdot A_{plas} \cdot f_u - k_{out} \cdot A_{tis} + k_{off} \cdot A_{tis,deep} - k_{on} \cdot A_{tis} \quad (2)$$

where A_{tis} = amount in tissue, A_{plas} = amount in plasma, $A_{tis,deep}$ = amount in deep compartment connected to tissue, k_{in} = rate constant for uptake in tissue/PML, k_{out} = rate constant for distribution out of tissue/PML, and k_{on}/k_{off} = on and off rate constants in tissue/PML compartments.

In addition, the model was validated using a VPC against external individual plasma, PML, and PBM data. PML and PBM concentrations were assumed to be similar based on data from Sampson *et al.*, 2014.[7]

Third, once the improvement of plasma and PML/PBM predictions was completed, development then focused on the extension of the model to predict concentrations in lung tissue and AMs (**Figure 1**). The lung compartment was parameterized assuming unit density (1 g/cm^3) when comparing lung predictions with digitized lung concentrations.[8,10,11] Extension of the model to AMs assumed a similar description regarding intracellular concentrations as that described in PMLs after adjusting for distribution in lung tissue. These compartments shared the parameters used for distribution into

tissue and cell compartments from the base model and are shown in Eq. 3 for change in drug in lung over time (dA_{lung}/dt) and Eq. 4 for change in AM over time (dA_{AM}/dt):

$$\frac{dA_{lung}}{dt} = k_{in} \cdot A_{plas} \cdot f_u - k_{out} \cdot A_{lung} + k_{off} \cdot A_{lung,deep} - k_{on} \cdot A_{lung} \quad (3)$$
$$+ k_{out} \cdot A_{AM} - k_{in} \cdot A_{lung} \cdot f_{unionized}$$

$$\frac{dA_{AM}}{dt} = k_{in} \cdot A_{lung} \cdot f_{unionized} - k_{out} \cdot A_{AM} + k_{off} \cdot A_{AM,deep} - k_{on} \cdot A_{AM} \quad (4)$$

where the parameter $f_{unionized}$ is calculated based on AZ pK$_a$ (pK$_{a1}$: 8.1, pK$_{a2}$: 8.8) and physiologic pH as reported in Zheng *et al.*,[5] using the same assumption that plasma and tissue compartment pH are similar, and k_{in}, k_{out}, k_{off}, k_{on}, and A_{plas} have been defined above. The rate constants of distribution into and out of the lung and AMs (k_{in}/k_{out} ratios) were assumed to be the same as muscle/subcutis and PMLs, respectively. It should be noted that this assumption does not cover all distribution parameters, as these rate parameters were allowed to scale with the estimation of a distribution factor.

A local sensitivity analysis was performed to assess the sensitivity of area under the concentration-time curve (AUC) in AM and lung tissue to changes in model parameters. Parameters were perturbed by up to ± 20% with 2% intervals (−20%, −18%, −16%, etc.) to simulate AUC and were compared against the reference AUC simulated from unperturbed parameters.

Model simulations were conducted using the R statistical and programming language (version 3.6.1) with mrgsolve and tidyverse packages.[18–20] Models implemented in mrgsolve were compared against NONMEM (version 7.4.3)[21] to validate model specifications. Visual evaluation was used to

assess models during development, consisting of: (i) comparison of simulated typical model predictions against digitized mean and SD data in plasma, lungs, muscle, subcutis, AMs, PBMs, and PMLs; (ii) VPC using individual clinical plasma concentration data; and (iii) VPC using individual clinical WBC concentration data. VPCs were generated by simulating from the observed data 1,000 times, with the median 50th, 5th, and 95th percentiles of the individual predictions from each simulation and 95% prediction intervals presented with an overlay of the observed data in those tissues.

Data for external validation

Data used for model evaluation included digitized aggregate tissue data from literature and individual clinical trial data. Digitized tissue data were collected from eight different studies as reported in the literature,[5–13] which consisted of mean and SD values over time for six unique dosing regimens. **Table 1** presents tissue/cell concentrations and a high-level summary of the study designs that were available from each literature source.

Individual clinical trial data were available from two published phase I studies.[9,22] The first study used an open-label randomized single dose design ($n = 40$), to estimate the bioavailability of a fixed dose combination of AZ-chloroquine tablets relative to co-administration of separate AZ and chloroquine tablets.[22] These formulations were considered bioequivalent based on the conclusions of the study.

The second study, already mentioned above, was an open-label randomized parallel-group study ($n = 24$) comparing the plasma, PML, and MNL pharmacokinetics (PKs) of AZ single-dose sustained release AZ (2 g) and a 3-day regimen of immediate release AZ (3 × 500 mg).[9] Only the immediate release data ($n = 12$) were used in the present analysis.

Model simulations and companion app

The final model was used for simulations of drug concentrations based on planned AZ dosing regimens in COVID-19 clinical trials, as reported on registry clinicaltrials.gov (accessed on April 8, 2020; **Supplementary Table S2**). Simulations consisted of 1,000 individuals, with median predictions and 90% prediction intervals in plasma, PMLs/PBMs, lung tissue, and AMs compared with the EC_{90} (8.65 μM) of AZ against SARS-CoV-2.

A companion app was also developed for the simulation of AZ concentrations in relevant tissues using a variety of different dosing regimens (https://github.com/jhhughes256/azithro_pk). The application was designed to allow for individual and population simulations, user-defined dosing regimens, comparison of predictions between different dosing regimens, adjustment of EC_{90} values, and assessment of time above the EC_{90} in lungs and AMs.

RESULTS
Model development

Implementation and evaluation of the initial base model developed by Zheng *et al.*[5] highlighted differences in the modeled population, with parameter estimates and typical predictions differing substantially from AZ plasma/serum profiles reported by Zhao *et al.*[14] (**Supplementary Figure S1.1**) and by Liu *et al.*[9] (**Supplementary Figure S1.2**),

and PML and MNL concentrations by Liu *et al.*[9] (**Supplementary Figure S1.3**). The estimate of total apparent clearance (CL/F) was reported as 258 L/hour (bootstrap 95% confidence interval (CI) 71–517) by Zheng *et al.* and was derived based on a small number of subjects ($N = 6$).[5] Although not directly comparable to the CL/F estimates for PopPK models of total plasma concentrations, when accounting for f_u (~ 0.5–0.9) the CL/F estimate (129–232 L/hour) was equal or greater than other reported PopPK values (range 100–158 L/hour; **Supplementary Table S1**). To adjust for the misspecification against external central tendencies, the parameters describing the systemic disposition of AZ including absorption were updated using data reported by Zhao *et al.*[14] The Zhao *et al.*[14] model was selected as the

Table 2 Pharmacokinetic parameters of the base, hybrid, and final models

	Base model[5]	Hybrid model[5,14]	Final model
Fixed effect parameters			
T_{lag}, hour	1.45	-	-
k_a, hour^{-1}	0.88	0.259	0.259
CL/F, L/hour	258	100	100
Normalization for body weight	NA	0.75	0.75
V_c/F, L	160	186	186
Normalization for body weight	NA	1.00	1.00
Q_{P1}/F, L/hour	207	180	180
Normalization for body weight	NA	0.75	0.75
V_{P1}/F, L	1190	2490	2290
Normalization for body weight	NA	1.00	1.00
Q_{P2}/F, L/hour	101	10.6	10.6
V_{P2}/F, L	9721	2610	2610
k_{in}, hour^{-1}	0.16	0.16	0.16
k_{out}, hour^{-1}	0.15	0.15	0.15
k_{on}, hour^{-1}	0.56	0.56	0.56
k_{off}, hour^{-1}	0.05	0.05	0.05
DF_{muscle}	0.55	0.55	0.55
$DF_{subcutis}$	0.25	0.25	0.25
$DF_{PML/WBC(cytosol)}$	52	52	77
DF_{lung}	-	-	140
$DF_{AM(cytosol)}$	-	-	730
Interindividual variability (%CV)			
T_{lag}	17.6	-	-
CL/F	29.3	31.3	31.3
V_c/F	168.3	113	113
k_{in}	0.22	0.22	0.22
DF_{muscle}	26.9	26.9	26.9
$DF_{subcutis}$	31.5	31.5	31.5
$DF_{PML/WBC(cytosol)}$	0.22	0.22	0.22

CL/F, apparent clearance; CV, coefficient of variation; DF, distribution factor; k_a, first-order absorption rate constant; k_{in}, rate constant for uptake into tissue compartments; k_{on} and k_{off}, rate constants for nonspecific tissue binding; k_{out}, rate constant for distribution out of tissue; NA, not applicable; Q_{P1}/F, apparent fast peripheral intercompartment clearance; Q_{P2}/F, apparent slow peripheral intercompartment clearance; T_{lag}, absorption lag; V_c/F, apparent central volume of distribution; V_{P1}/F, apparent fast peripheral volume of distribution; V_{P2}/F, apparent slow peripheral volume of distribution.

ideal candidate due to its three-compartment structure, number of subjects included in the analysis, robustness of the analysis, and inclusion of weight as a covariate enabling predictions in other populations. Mean parameter estimates were similar to the other reported values (**Supplementary Table S1**).

When implementing the parameters from the Zhao *et al.* three-compartment model, the apparent volume of distribution in the fast distributing compartment was corrected (2890 L to 2490 L) to account for the added volume of 400 L attributed to the addition of both the muscle and subcutis compartments. The value was derived based on K_{in} and K_{out} values reported by Zheng *et al.*[5] The combination of parameters in the hybrid model (**Table 1**) provided adequate prediction of both the digitized data from Zheng *et al.* (**Supplementary Figure S2**) and the observed data used in development of the Zhao *et al.* model[14] used as internal validation.

Model predictions from the hybrid model were also validated against mean reported values of both PMLs and PBMs.[7,9,13] The pooled white blood cell (WBC; either PML or PBM) predictions used total concentrations in WBCs, which included both ionized (major component in cells) drug in lysosomes and un-ionized drug in cytosol. As the model predictions for the pooled WBC compartment tended to underestimate the concentrations of different PBM/PML data sources (not shown), the distribution factor for the pooled WBC cytosol was increased from 52 to 77. This final estimate was contained within the reported bootstrap CIs of the

distribution factor estimate for PML cytosol (95% CI 39–423)[5] and this adjustment visually improved model predictions.

As described in Methods, the hybrid model was extended to represent the lung tissue and AM cells (**Figure 1**). Volume displacement caused by adding the lung compartment was accounted for by reducing the apparent fast-distributing peripheral compartment, as described previously. The initial values for distribution factors to the new lung and AM compartments were determined by calculating the ratio between tissue and plasma from Lucchi *et al.*[8] and Danesi *et al.*[10] and further adjusted based on visual evaluation. The final model parameters are presented in **Table 2** and code provided in the **Supplementary Material**. VPC of the individual serum and WBC (observed PML and MNL) concentrations[9] are shown in **Figure 2** and supported the validity of the final model.

Results of the local sensitivity analysis in AM and lung tissue (not shown) demonstrated that AUC was highly sensitive to the value of CL/F and the distribution factor for the respective tissues. AUC in AMs was also sensitive to changes in k_{in} and k_{out}. These parameters were shared with the PML compartment, assuming a similar ratio between distribution into and out of both cell types, with the scalar distribution factor controlling the magnitude of the rate of distribution. Although the sensitivity of AUC to changes in k_{in} and k_{out} supported estimation of tissue-specific values for these parameters, there was insufficient data to support determination of all three sensitive parameters (k_{in}, k_{out}, and distribution factor$_{AM}$). As the main difference between PML and AM concentration profiles were the
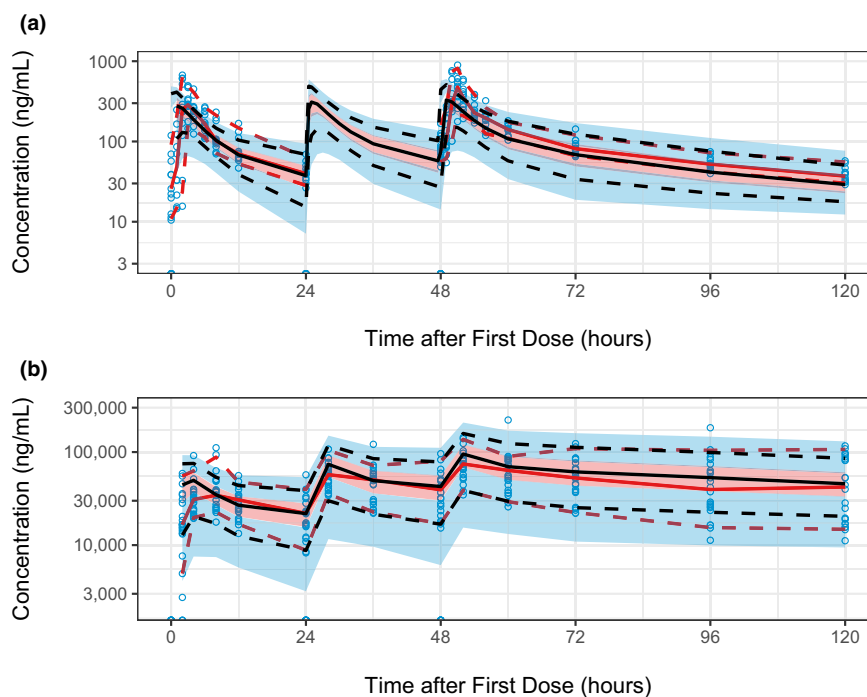
Figure 2 Visual predictive checks of the final model for azithromycin concentrations in plasma (**a**) and white blood cell (**b**) using external data from Liu *et al.*[9] The observed azithromycin concentrations are represented by blue circles, whereas the median, 5th, and 95th percentiles of the observed data are represented by the solid, lower-dashed, and upper-dashed red lines. The median, 5th, and 95th percentiles of predictions from 1,000 simulations of the observed data are represented by the solid, lower-dashed, and upper-dashed black lines. The 95% prediction intervals for the median, 5th, and 95th percentiles of the simulated data are represented by the red, lower-blue, and upper-blue shaded areas.
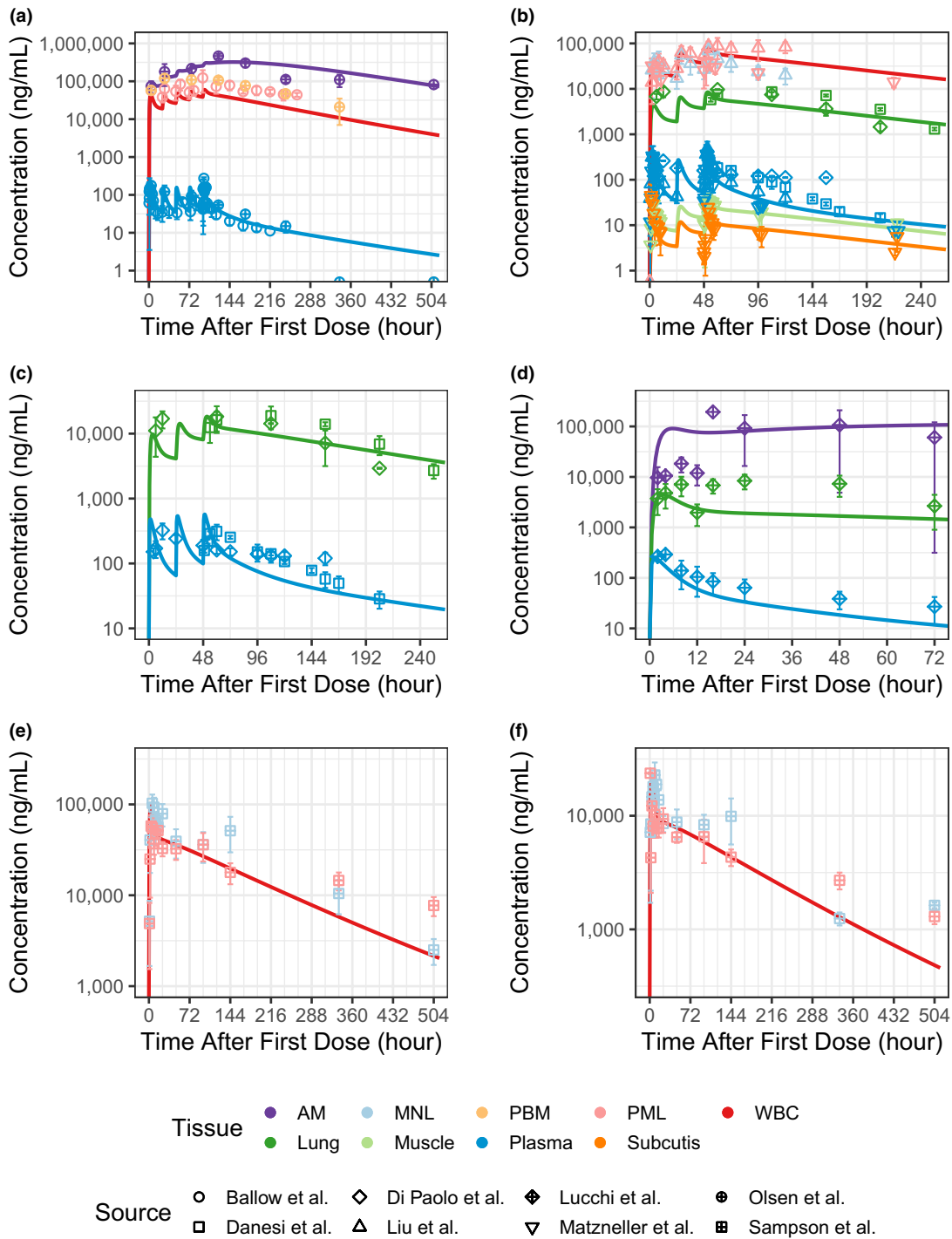
Figure 3 Comparison of final model predictions with digitized literature values. The digitized mean and SDs from literature data are represented by the shapes and error bars respectively. The solid lines represent the typical simulated predictions in different tissues when simulating patients (body weight 79 kg) treated with azithromycin: (**a**) 500 mg initial dose, followed by 250 mg daily for 4 days; (**b**) 500 mg daily for 3 days; (**c**) 1,000 mg daily for 3 days; (**d**) 500 mg single dose; (**e**) 1,000 mg single dose; and (**f**) 250 mg single dose. AM, alveolar macrophage; MNL, morphonuclear leukocyte; PBM, peripheral blood monocyte; PML, polymorphonuclear leukocyte; WBC, white blood cell.

magnitude of the concentrations, no changes were made to the underlying assumptions of the model based on the sensitivity analysis.

As shown in **Figure 3**, the final model adequately described the mean systemic (plasma/serum), pooled WBC, tissue (muscle and subcutis), lung, and AM concentrations

(a)

(b)

(c)

(d)

Tissue — AM — Lung — Plasma — WBC
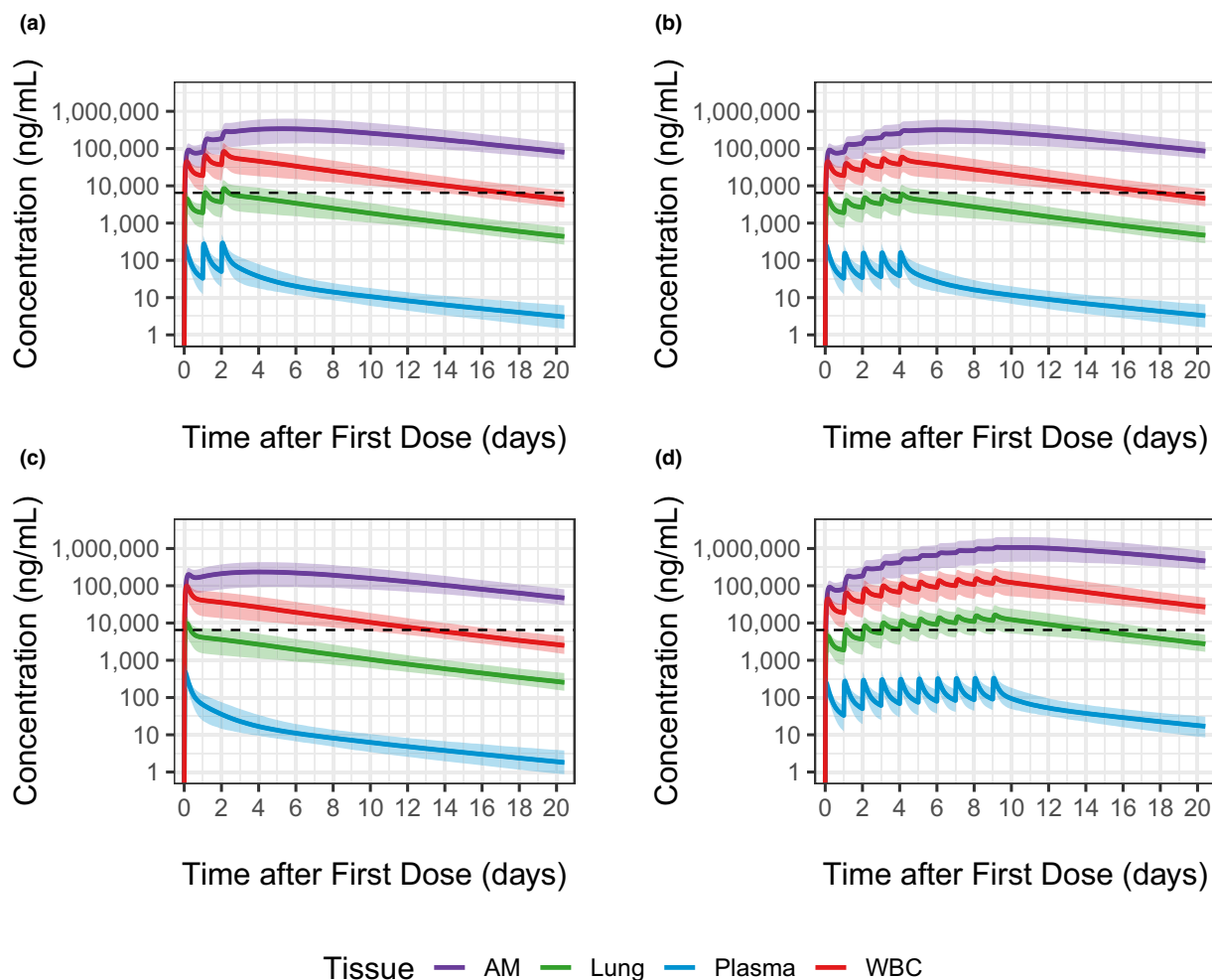
Figure 4 Final model simulation of azithromycin concentrations for different treatment regimens. Treatment regimens were: (**a**) 500 mg daily for 3 days; (**b**) 500 mg initial dose, followed by 250 mg daily for 4 days; (**c**) 1,000 mg single dose; and (**d**) 500 mg daily for 10 days. Solid lines represent the median concentration from 1,000 simulated individuals (body weight 79 kg), while shaded areas represent the 90% prediction intervals. Black dashed line represents *in vitro* 90% inhibitory concentration.

across different studies using different dosing regimens. The model was sufficiently robust to describe the AZ PKs following single dose administration (doses of 250, 500, and 1,000 mg), 3-day regimen (500 and 1,000 mg), and the commonly used regimen of 500 mg on day 1 followed by 250 mg days 2 to 5.

Model simulations

Based on the most commonly reported dosing regimens for AZ investigated in clinical trials of COVID-19 (**Supplementary Table S2**), systemic concentrations, total concentrations in lung tissue, and intracellular concentrations in PML/PBM and AM, were predicted and compared against the reported 90% inhibitory concentration (IC_{90}) for antiviral activity *in vitro* (**Figure 4**). Consistent with known properties of AZ, drug concentrations were higher intracellularly as shown in AM and WBC (PBM/PML), followed by lung tissue and plasma. Concentrations in WBC exceeded the *in vitro* IC_{90} starting

following first dose and for ~ 14 days with either of the currently approved regimens for bacterial pulmonary infections (500 mg q.d. days 1–3 or 500 mg on day 1, followed by 250 mg q.d. days 2–5), 10 days following a single 1,000 mg dose, and > 20 days with administration of 500 mg q.d. for 10 days. Trough concentrations in AM were ~ 4-fold greater than those in WBC after first dose and exceeded the IC_{90} for > 20 days based on the four regimens tested. Concentrations in total lung tissue were generally below IC_{90} except following administration of 500 mg q.d. for 10 days.

DISCUSSION

As the world faces the COVID-19 pandemic with a rapidly growing number of individuals infected, the demand for therapeutics against SARS-COV-2 is most urgently met by repurposing approved compounds and evaluating their activity against the virus. The use of hydroxychloroquine

in this population has been extensively covered by the press, and different quantitative approaches have been implemented to support its use, including a physiologically-based pharmacokinetic model,[23] a PK/virologic/corrected QT model,[24] and a web application quantifying exposure (http://www.covid19pkpd.eu/simulator/). *In vitro* screening of a chemical library of compounds identified activity of a selected number of drugs against SARS-COV-2 replication, including AZ with a potent 50% effective concentration of 2.12 μM.[4] To further support the rationale for evaluation of AZ in these patients, a PK model was developed based on an existing semi-physiologic model and existing tissue data to predict intracellular concentrations.

Modeling of the viral dynamics of SARS-CoV-2 described in a recent preprint by Gonçalves *et al.* identified that treatment either initiated at the time of infection, symptom onset, or 3 days post-symptom onset would require at least a 60%, 90%, or 99% efficacy in reducing viral replication, respectively, to reduce the peak viral load by > 2 log units.[25] According to the work presented herein, predicted AZ in AMs and WBCs exceeded the *in vitro* EC$_{90}$ for AZ against SARS-CoV-2. Providing that these cells represent the site of action against SARS-CoV-2, AZ may be effective even after starting treatment up to 3 days after symptom onset. However, if the lung tissue better represents effective concentration at the site of action, then treatment would need to be initiated prior to or during symptom onset.

Simulations of the final model show that AZ accumulates in intracellular compartments (AM and PBM/PML), with slow distribution out of these cells over time. As a result, the extent of exposure in these cells is dependent on the total dose administered regardless of regimen. The 3-day and 5-day regimens with a total dose of 1.5 g provided similar profiles in these compartments, whereas lower exposure was noted with 1 g administered as a single dose and higher exposure noted with 5 g administered over 10 days. Considering the large number of possible dosing regimens and the assumptions that can be made regarding clinical effectiveness, the model, analysis, and web application code have been provided for researchers to analyze different dosing scenarios other than those included herein (https://github.com/jhhughes256/azithro_pk).

One limitation of the approach used for implementation of the present model was the use of data collected in healthy volunteers, whereas lung data was obtained in patients without infection undergoing lung resection. In the presence of viral infection, distribution in lung tissue may be increased, and, thus, the model may underestimate lung concentrations in infected individuals. Despite this limitation, the present analysis and web application enables the evaluation of alternate scenarios, and will better inform optimization of dosing regimens for ongoing and future AZ clinical trials.

Supporting Information. Supplementary information accompanies this paper on the *CPT: Pharmacometrics & Systems Pharmacology* website (www.psp-journal.com).

1. Gautret, P. *et al*. Hydroxychloroquine and azithromycin as a treatment of COVID-19: results of an open-label non-randomized clinical trial. *Int. J. Antimibrob. Agents.* 10.1016/j.ijantimicag.2020.105949. [e-pub ahead of print].
2. Gautret, P. *et al*. Clinical and microbiological effect of a combination of hydroxychloroquine and azithromycin in 80 COVID-19 patients with at least a six-day follow up: an observation study. *Travel Med. Infect. Dis.* 10.1016/j.tmaid.2020.101663. [e-pub ahead of print].
3. Damle, B., Vourvahis, M., Wang, E., Leaney, J. & Corrigan, B. Clinical pharmacology perspectives on the antiviral activity of azithromycin and use in COVID-19. *Clin. Pharmacol. Therapeut.* https://doi.org/10.1002/cpt.1857. [e-pub ahead of print].
4. Touret, F.*et al*.In vitro screening of a FDA approved chemical library reveals potential inhibitors of SARS-CoV-2 replication. *bioRxiv*. 10.1101/2020.04.03.023846. [epub ahead of print].
5. Zheng, S., Matzneller, P., Zeitlinger, M. & Schmidt, S. Development of a population pharmacokinetic model characterizing the tissue distribution of azithromycin in healthy subjects. *Antimicrob. Agents Chemother.* **58**, 6675–6684 (2014).
6. Matzneller, P. *et al*. Blood, tissue, and intracellular concentrations of azithromycin during and after end of therapy. *Antimicrob. Agents Chemother.* **57**, 1736–1742 (2013).
7. Sampson, M.R., Dumitrescu, T.P., Brouwer, T.P. & Schmith, V.D. Population pharmacokinetics of azithromycin in whole blood, peripheral blood mononuclear cells, and polymorphonuclear cells in healthy adults. *CPT Pharmacometrics Syst. Pharmacol.* **3**, e103 (2014).
8. Lucchi, M. *et al*. Pharmacokinetics of azithromycin in serum, bronchial washings, alveolar macrophages and lung tissue following a single oral dose of extended or immediate release formulations of azithromycin. *J. Antimicrob. Chemother.* **61**, 884–891 (2008).
9. Liu, P. *et al*. Comparative pharmacokinetics of azithromycin in serum and white blood cells of healthy subjects receiving a single-dose extended-release regimen versus a 3-day immediate-release regimen. *Antimicrob. Agents Chemother.* **51**, 103–109 (2007).
10. Danesi, R. *et al*. Comparative distribution of azithromycin in lung tissue of patients given oral daily doses of 500 and 1000 mg. *J. Antimicrob. Chemother.* **51**, 939–945 (2003).
11. Di Paolo, A., Barbara, C., Chello, A., Angeletti, C.A. & Del Tacca, M. Pharmacokinetics of azithromycin in lung tissue, bronchia washing, and plasma in patients given multiple oral doses of 500 and 1000 mg daily. *Pharmacol. Res.* **46**, 545–550 (2002).
12. Ballow, C.H., Amsden, G.W., Highet, V.S. & Forrest, A. Pharmacokinetics of oral azithromycin in serum, urine, polymorphonuclear leucocytes and inflammatory vs non-inflammatory skin blisters in healthy volunteers. *Clin. Drug Invest.* **15**, 159–167 (1998).
13. Olsen, K.M., San Pedro, G., Gann, L.P., Gubbins, P.O., Halinski, D.M. & Campbell, G.D. Jr Intrapulmonary pharmacokinetics of azithromycin in healthy volunteers given five oral doses. *Antimicrob. Agents Chemother.* **40**, 2582–2585 (1996).
14. Zhao, Q., Tensfeldt, T.G., Chandra, R. & Mould, D.R. Population pharmacokinetics of azithromycin and chloroquine in healthy adults and paediatric malaria subjects following oral administration of fixed-dose azithromycin and chloroquine combination tablets. *Malaria J.* **13**, 36 (2014).
15. Dumitrescu, T. *et al*. Development of a population pharmacokinetic model to describe azithromycin whole-blood and plasma concentrations over time in healthy subjects. *Antimicrob. Agents Chemother.* **57**, 3194–3201 (2013).
16. Salman, S. *et al*. Pharmacokinetic properties of azithromycin in pregnancy. *Antimicrob. Agents Chemother.* **54**, 360–366 (2010).
17. Zhang, X.Y., Wang, Y.R., Zhang, Q. & Lu, W. Population pharmacokinetics study of azithromycin oral formulations using NONMEM. *Int. J. Clin. Pharmacol. Ther.* **48**, 662–669 (2010).
18. R Core Team. R: A Language and Environment for Statistical Computing. R Foundation for Statistical Computing, Vienna, Austria (2019). <https://www.R-project.org/>.
19. Baron, K.T. mrgsolve: Simulate from ODE-Based Models. R package version 0.9.2. <https://CRAN.R-project.org/package=mrgsolve> (2019).
20. Wickham, H. tidyverse: easily install and load the 'Tidyverse'. R package version 1.2.1. <https://CRAN.R-project.org/package=tidyverse> (2017).
21. Beal, S., Sheiner, L.B., Boeckmann, A. & Bauer, R.J. NONMEM User's Guides (1989–2017). (ICON Development Solutions, Gaithersburg, MD, 2017).

22. Zhao, Q., Purohit, V., Cai, J., LaBadie, R. & Chandra, R. Relative bioavailability of a fixed-combination tablet formulation of azithromycin and chloroquine in healthy adult subjects. *J. Bioequivalence Bioavailab.* **5**, 1–5 (2013).

23. Yao, X. *et al.* In vitro antiviral activity and projection of optimized dosing design of hydroxychloroquine for the treatment of Severe Acute Respiratory Syndrome Coronavirus 2 (SARS-CoV-2). *Clin. Infect. Dis.* 10.1093/cid/ciaa237. [epub ahead of print].

24. Garcia-Cremades, M. *et al.* Optimizing hydroxychloroquine dosing for patients with COVID-19: an integrative modeling approach for effective drug repurposing. *Clin. Pharmacol. Therapeut.* 10.1002/cpt.1856. [epub ahead of print].

25. Gonçalves, A. *et al.* Timing of antiviral treatment initiation is critical to reduce SARS-Cov-2 viral load. medRxiv. 10.1101/2020.04.04.20047886. [epub ahead of print].